ARTICLES SCIENCE CHINA Materials

mater.scichina.com link.springer.com

Published online 29 March 2016 | doi: 10.1007/s40843-016-0130-1
*Sci China Mater* 2016, 59(3): 182–190

SPECIAL ISSUE: Emerging Investigators of Nanomaterials

# Controlled synthesis of high-quality crystals of monolayer $MoS_2$ for nanoelectronic device application

Xiaonian Yang[1†], Qiang Li[2†], Guofeng Hu[1†], Zegao Wang[2], Zhenyu Yang[3], Xingqiang Liu[1], Mingdong Dong[2] and Caofeng Pan[1*]

**ABSTRACT Two-dimensional layered materials have attracted significant interest for their potential applications in electronic and optoelectronics devices. Among them, transition metal dichalcogenides (TMDs), especially molybdenum disulfide ($MoS_2$), is extensively studied because of its unique properties. Monolayer $MoS_2$ so far can be obtained by mechanical exfoliation or chemical vapor deposition (CVD). However, controllable synthesis of large area monolayer $MoS_2$ with high quality needs to be improved and their growth mechanism requires more studies. Here we report a systematical study on controlled synthesis of high-quality monolayer $MoS_2$ single crystals using low pressure CVD. Large-size monolayer $MoS_2$ triangles with an edge length up to 405 μm were successfully synthesized. The Raman and photoluminescence spectroscopy studies indicate high homogenous optical characteristic of the synthesized monolayer $MoS_2$ triangles. The transmission electron microscopy results demonstrate that monolayer $MoS_2$ triangles are single crystals. The back-gated field effect transistors (FETs) fabricated using the as-grown monolayer $MoS_2$ show typical n-type semiconductor behaviors with carrier mobility up to 21.8 $cm^2 V^{-1} s^{-1}$, indicating excellent electronic property comparing with previously reported CVD grown $MoS_2$ monolayer. The $MoS_2$ FETs also show a high photoresponsivity of 7 A $W^{-1}$, as well as a fast photo-response time of 20 ms. The improved synthesis method recommended here, which makes material preparation much easier, may strongly promote further research and potential applications.**

**Keywords:** controlled synthesis method, high-quality $MoS_2$ monolayer, growth parameters, photoresponse properties

## INTRODUCTION

Two-dimensional (2D) layered transition metal dichalcogenides (TMDs) have attracted tremendous attention in recent years owing to their unique properties and potential applications in the next generation electronic and optoelectronics devices [1–3]. Typically, TMDs semiconductors have an indirect band gap in bulk and would transform into direct band gap semiconductor when they become monolayer, which gives them great advantages over zero band gap graphene. Monolayer molybdenum disulfide ($MoS_2$), with a direct band gap of 1.8 eV, is one of the most extensively studied TMDs materials because of its superior electronic properties and potential applications in nanodevices [4–9]. Previous studies also show its excellent physical and chemical properties, including ferroelectric gating, piezoelectronic and gas-sensitive properties [10–15]. Like other 2D materials, monolayer $MoS_2$ can be obtained via traditional mechanical exfoliation as well as chemical vapor deposition (CVD) method [16–21]. While mechanical exfoliated monolayer $MoS_2$ flakes display excellent electronic and optoelectronic properties, the small size and the low production of these monolayer $MoS_2$ flakes hinder them from further development. Synthesis of large-area $MoS_2$ films have been reported in the past few years [22–27]. However, the preparation of large-size monolayer $MoS_2$ single crystals remain to be improved in view of its superior electronic and optoelectronic characteristics [28–31]. Furthermore, as the size of $MoS_2$ single crystals increased to hundreds of micrometers, the device fabrication and modulation process would be simplified greatly. Moreover, controllable synthesis of large-size monolayer $MoS_2$ single crystals is an important step toward practical applications

[1] Beijing Institute of Nanoenergy and Nanosystems, Chinese Academy of Sciences, Beijing 100083, China
[2] Interdisciplinary Nanoscience Center (iNANO), Aarhus University, DK 8000 Aarhus C, Denmark
[3] Department of Physics and Key Laboratory of Artificial Micro- and Nano-structures of Ministry of Education, Wuhan University, Wuhan 430072, China
[†] These authors contributed equally to this work.
[*] Corresponding author (email: cfpan@binn.cas.cn)

of $MoS_2$.

Here, we report a systematical study on low-pressure CVD growth of high-quality crystals of monolayer $MoS_2$ with grain sizes up to 405 μm, which also possess optical and electrical properties comparable to those of exfoliated $MoS_2$ samples. The optical properties of the as-synthesized monolayer $MoS_2$ were characterized using Raman and photoluminescence (PL) spectroscopies. High-resolution transmission electron microscopy (TEM) was then employed to carefully observe the crystal structures of the monolayer $MoS_2$. Finally, plenty of back-gated field effect transistors (FETs) were fabricated to characterize the electronic and optoelectronic properties of the as-synthesized large-size crystals of monolayer $MoS_2$. The calculated mobility of the $MoS_2$ FETs was measured up to 21.8 $cm^2 V^{-1}s^{-1}$, which is higher than many previously reported CVD grown $MoS_2$ monolayers. The $MoS_2$ FETs also show a good photoresponsivity of 7 A $W^{-1}$, as well as a fast photo-response time of 20 ms. These results suggest that the large-size crystals of monolayer $MoS_2$ grown by our improved CVD methods may strongly promote further research and potential applications.

## EXPERIMENTAL SECTION

### Growth of monolayer $MoS_2$

The monolayer $MoS_2$ was grown from $MoO_3$ and sulfur on a clean Si substrate with 300 nm $SiO_2$ in a traditional tube furnace under low pressure conditions. The schematic of the synthesis system is shown in Fig. 1a. A quartz boat carrying 100 mg $MoO_3$ powder (99.95%, Alfa Aesar) was placed in the middle of the heating zone of the reacting furnace. A clean Si substrate with 300 nm-thick $SiO_2$ layer was placed face down on the top of the quartz boat. Another quartz boat containing 150 mg sulfur pieces (99.999%, Alfa Aesar) was placed near the argon inlet end. $MoO_3$ and sulfur pieces were heated to the reaction temperature and the argon acted as the carrier gas. The furnace temperature was first raised up to 120°C and kept for 30 min. Then the $MoO_3$ powder was heated to the reaction temperature at the rate of 30°C $min^{-1}$. When the growth temperature was reached, the sulfur pieces were heated to 150°C. During the whole growth process, argon flow of 50 sccm was used to provide an inert atmosphere and carry the vapors of the precursor. Once the growth was finished, the system was quickly cooled down to room temperature.

To synthesize large-size high-quality crystals of monolayer $MoS_2$, we performed a series of CVD growth parameters and found the optimal parameter. According to previous studies on synthesis of monolayer TMDs and our experiments [28,32,33], growth temperature, inner pressure of the furnace tube, and growth durations are the three main parameters that significantly influence the quality of the as-grown $MoS_2$. In this case, the growth temperatures were adjusted in a range of 750 to 950°C, while the inner pressures of the furnace were changed from 0.5 to 10 kPa.

### Raman and photoluminescence characterization

The Raman and PL spectroscopy measurements were performed via an Andor 500i spectrograph with a 532 nm laser. The Raman curves were taken using a 1200 l $mm^{-1}$ grating for 30 s, while the PL curves were taken with a 600 l $mm^{-1}$ grating for 20 s. The Raman and PL mapping were conducted on the same instrument with the same laser line.

### TEM sample preparation and characterization

A typical Cu micro grid was selected to carry the monolayer $MoS_2$ samples. A 70 nm polymethyl methacrylate (PMMA) layer was spin-coated on the surface of $MoS_2$ samples on the $SiO_2$/Si substrate. Then the substrate was put into 2 mol $L^{-1}$ KOH solution to remove the substrate through etching the $SiO_2$ epilayer and leave the PMMA film with $MoS_2$ monolayers floating on the surface. The film was then transferred onto the Cu micro grid after several times of washing in deionized water and dried. Finally, the PMMA layer was removed by heating the Cu micro grid at 300°C for 6 h with an argon gas flow at atmospheric pressure.

### Device fabrication and measurement

The back-gated monolayer $MoS_2$ FETs were fabricated directly on the $SiO_2$/Si substrates. Firstly, a PMMA layer of 200 nm was spin-coated on the surface of the monolayer $MoS_2$. Electron beam lithography was then employed to pattern the electrical contacts to $MoS_2$. Then 5 nm Ti and 50 nm Au were deposited by E-beam evaporation. The $MoS_2$ FETs were measured under ambient conditions using the silicon substrate as a back gate. All the electrical and photo-response properties were characterized using a Keithley 4200S semiconductor analysis instrument.

## RESULTS AND DISCUSSION

The growth durations mainly affect the grain sizes and growth density of $MoS_2$, so different reaction times were performed to find the most suitable growth time. Figs 1b and c show the optical images of monolayer $MoS_2$ grown at optimized parameter. As can be seen, $MoS_2$ flakes exhibit uniform triangular shape with edge lengths in the range of 50–250 μm (Fig. 1b). Across different growths, the average edge lengths of triangle $MoS_2$ varies from 100 to 300 μm, with individual triangles up to 405 μm (Fig. 1c) which are

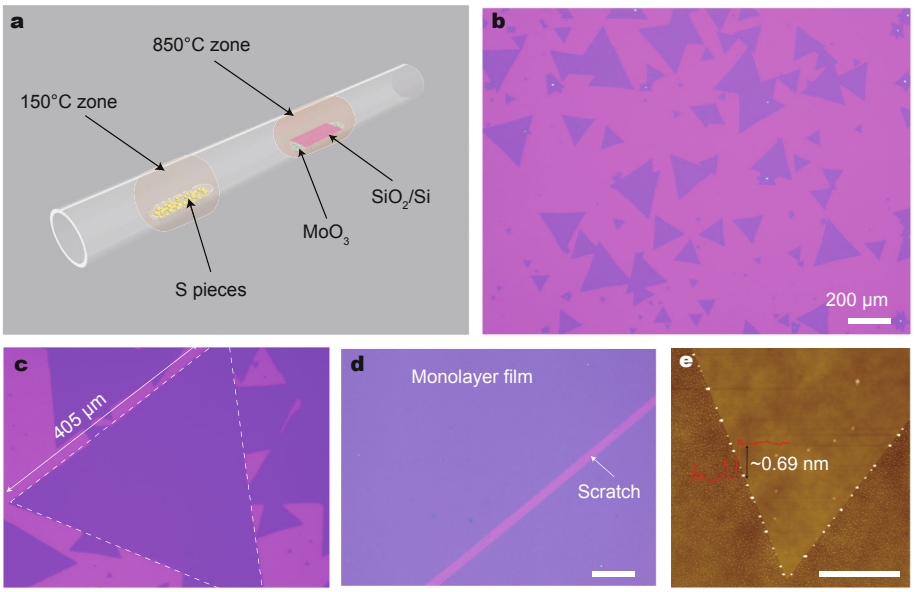


**Figure 1** Schematic of the synthesis and morphology characterization of the large-size monolayer $MoS_2$. (a) Schematic of the synthesis process for $MoS_2$. (b) A typical optical image of the as-synthesized monolayer $MoS_2$ triangles on $SiO_2$/Si substrate, the scale bar is 200 μm. (c) Optical image of a large-size monolayer $MoS_2$ triangle, the measured edge length is 405 μm. (d) Optical image of monolayer $MoS_2$ film with a tweezers' scratch, the scale bar is 50 μm. (e) AFM image of a monolayer $MoS_2$ triangle with a measured thickness of 0.69 nm, the scale bar is 2 μm.

significant larger than previous reported CVD grown $MoS_2$ triangles [17,28]. To the best of our knowledge, the $MoS_2$ triangle with edge length of 405 μm is the largest triangle reported so far. More importantly, our large-size $MoS_2$ triangles almost have no bilayers patches or multilayer nucleus, which indicates that the almost perfect monolayer $MoS_2$ triangles are likely to achieve extraordinary optical and electronic properties. Fig. 1d shows a continuous and homogeneous large-area $MoS_2$ film formed on the $SiO_2$/Si substrate, the tweezers' scratch on it made the fuchsia substrate be in sight. Fig. 1e is a typical atomic force microscopy (AFM) image which shows the step height of the $MoS_2$ triangle is about 0.69 nm. The measured height is in agreement with the thickness of the monolayer $MoS_2$, confirming that the as-grown $MoS_2$ triangles are monolayer.

In the present study, various growth parameters have been performed to explore the growth mechanism and to find the optimal parameter. Among the various growth behaviors, we highlighted the edge length of $MoS_2$ triangles, through which we could identify how the growth parameters functioned. Based on available literature and our previous systematical experiments [33], we found that growth temperature is the one influenced the most. Therefore, we firstly performed a systematic investigation of the influence of source temperature (mainly the temperature of $MoO_3$ powder) on the morphology of the as-grown $MoS_2$ at a tube pressure of 1 kPa and a fixed growth time of 10 min. In brief, sulfur pieces were put into a quartz boat near the argon inlet-end and a homemade heater was used to melt it, while another quartz boat carrying $MoO_3$ powder was located in the downstream of the furnace tube. The $SiO_2$/Si substrate was put on the quartz boat with $SiO_2$ side facing downwards. Argon was flowing at the rate of 50 sccm through the entire reaction.

At low source temperature (also the substrate temperature and reaction temperature) of 750°C, no visible $MoS_2$ monolayers can be observed on the substrate under optical microscope (Fig. 2a). However, there are tiny monolayers with edge lengths less than 1 μm come in sight when characterized with scanning electron microscope (SEM). When the temperature rose to 800°C, a great deal of monolayer $MoS_2$ triangles with average edge length of 35 μm are observed under the optical microscope (Fig. 2b). The size of the monolayer $MoS_2$ triangles keeps increasing as the reaction temperature reached 850°C. Uniform and morphology perfect monolayer $MoS_2$ triangles with average edge length of 203 μm distributed on the substrate were observed, as shown in Fig. 2c. However, as the temperature went on increasing to 900°C, the size of triangles did not tend towards larger. The average edge length of these triangles is about 90 μm (Fig. 2d), so is the triangles synthesized at the temperature of 950°C (Fig. 2e, the average edge length is about 50 μm). The summary of the edge length of $MoS_2$ triangles grown at different growth temperatures is shown in Fig. 2f.

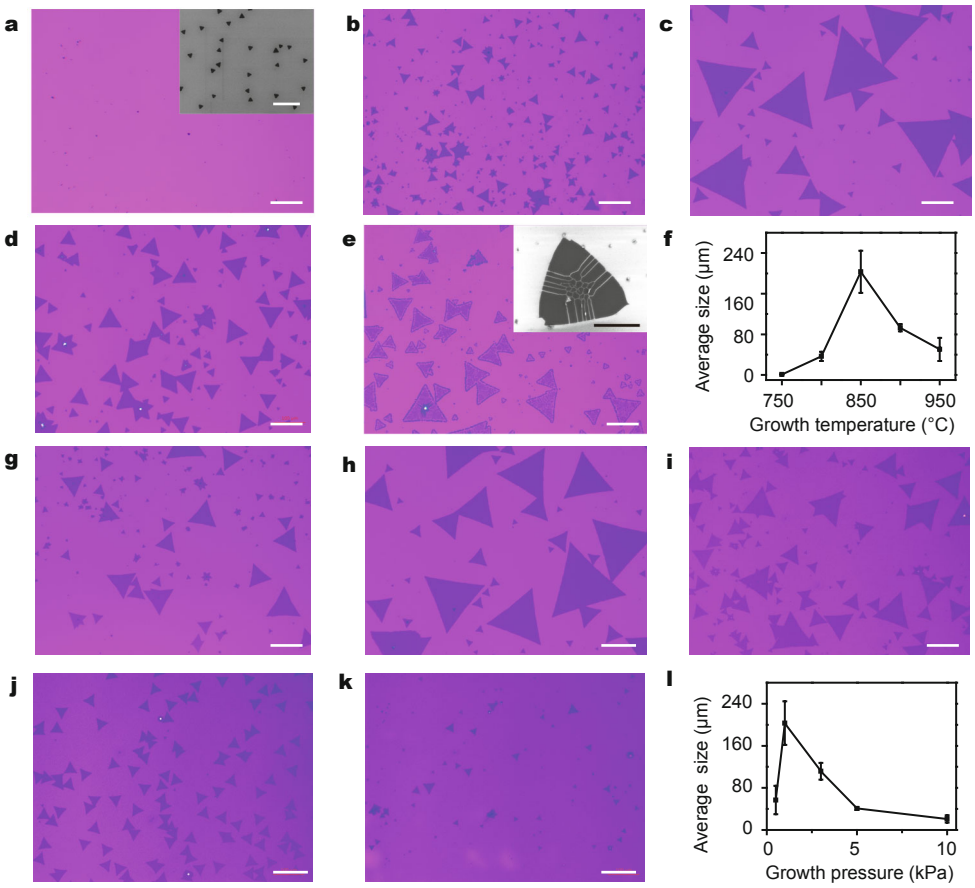


**Figure 2** Effects of growth temperature and pressure on the sizes of the monolayer $MoS_2$ triangles. (a–e) Optical images of $MoS_2$ samples grown at growth temperature of 750, 800, 850, 900 and 950°C, respectively. Scale bars are 100 μm. The inset in (a) is an SEM image, showing tiny $MoS_2$ triangles. The scale bar is 5 μm. The inset in (e) is an SEM image, showing cracks in monolayer $MoS_2$ triangles. The scale bar is 5 μm. (f) The correlation of average edge lengths of monolayer $MoS_2$ triangles with various growth temperatures. (g–k) Optical images of $MoS_2$ samples grown under tube pressure of 0.5, 1, 3, 5, 10 kPa, respectively. Scale bars are 100 μm. (l) The correlation of average edge length of monolayer $MoS_2$ triangles with different growth pressures.

As can be seen, the optimal growth temperature is around 850°C, with individual triangles up to 405 μm. These results also indicate that the higher source temperature makes the growth react more rapidly, as well as the sublimation rate of $MoO_3$. The higher reaction rate causes the triangles to grow faster, while higher sublimation rate may cause the $MoO_3$ vapor pressure lower since more reactant powder is sublimated and flows away before the reaction starts, which in turn leads to less nucleation density and smaller triangle size. Before the source temperature reaches 850°C, the reaction rates increasing with temperature impacts the reaction predominantly, and the size of triangles becomes larger with temperature increasing. When the temperature rises to 900°C and over, the main impact factor are the faster sublimation rate and lower $MoO_3$ vapor pressure, causing the size of the synthesized triangles smaller and many cracks occurred on the monolayer $MoS_2$ triangles (Fig. 2e, inset SEM image).

After the study of the optimal growth temperature, we then explored the influence of tube pressure on the monolayer $MoS_2$ triangles at the growth temperature of 850°C. As shown in Figs 2g–k, the tube pressure did have influence on the size of monolayer $MoS_2$ triangles. In general, with reaction temperature and other reaction parameters fixed, higher tube pressure leads to higher $MoO_3$ vapor pressure and higher concentration of crystal nucleus. Under lower tube pressure of 0.5 kPa, monolayer $MoS_2$ triangles with an average edge length of ~57 μm scattering on the substrate can be observed (Fig. 2g). By increasing the tube pressure to 1 kPa, the average size of the monolayer $MoS_2$ triangles increases to ~203 μm (Fig. 2h). The sizes of the monolayer triangles decrease to 112 μm while the tube pressure rising to 3 kPa (Fig. 2i). As the tube pressure reached 5 kPa, large amounts of multilayer nucleus and flakes appeared

on the middle of the growth substrate, with monolayer triangles (average edge size ~41 μm) grown on the edge of the growth substrate. Meanwhile, the density of monolayer $MoS_2$ triangles is higher (Fig. 2j). When the tube pressure reached 10 kPa, nearly the entire growth substrate was covered by multilayer flakes and bulk $MoS_2$ (Supplementary information, Fig. S1), only a handful of monolayer triangles (average edge size ~21 μm) can be observed on some marginal areas of the substrate (Fig. 2k). In general, the optimal tube pressure is 1 kPa at the growth temperature of 850°C and reaction time of 10 min. Lower tube pressure makes the $MoO_3$ power sublimates faster and leads to lower $MoO_3$ vapor pressure, thus reducing the $MoS_2$ nucleation density and the triangles' sizes. On the contrary, higher tube pressure increases the $MoS_2$ nucleation density and the triangles' sizes, while polycrystalline films and multilayer flakes may appear when the tube pressure is too high.

Spectroscopic techniques such as Raman and PL were employed to further characterize the quality of the as-grown $MoS_2$ samples. Fig. 3a shows five $MoS_2$ triangles with edge lengths of 60, 150, 190, 260 and 330 μm, respectively. These $MoS_2$ triangles were characterized using Raman and PL spectroscopies with a 532 nm laser. The Raman spectra results are shown in Fig. 3b. As can be seen, each Raman spectra has two obvious peaks, the in-plane vibrational mode $E^1_{2g}$ (at about 381.5 $cm^{-1}$) and the out-of-plane vibrational mode $A_{1g}$ (at about 402 $cm^{-1}$). The spectra curves corresponding to five different sizes of $MoS_2$ triangle samples show no obvious difference. The gap between $E^1_{2g}$ peak and $A_{1g}$ peak is 20.5 $cm^{-1}$, which is in consistent with previously reported gap of CVD grown monolayer $MoS_2$ triangles [34], indicating that the as-grown $MoS_2$ triangles are homogeneous monolayers, in spite of different sizes and different batches. The PL spectra examining results (Fig. 3c) of the five $MoS_2$ triangle samples all show strong peaks at the wavelength of about 683 nm, which is corresponding to the 1.82 eV direct band gap in monolayer $MoS_2$. Uniform Raman and PL mapping signals (Figs 3e and f, respectively) from a commonly selected individual $MoS_2$ triangle (Fig. 3d) further reveal the homogeneous nature of these $MoS_2$

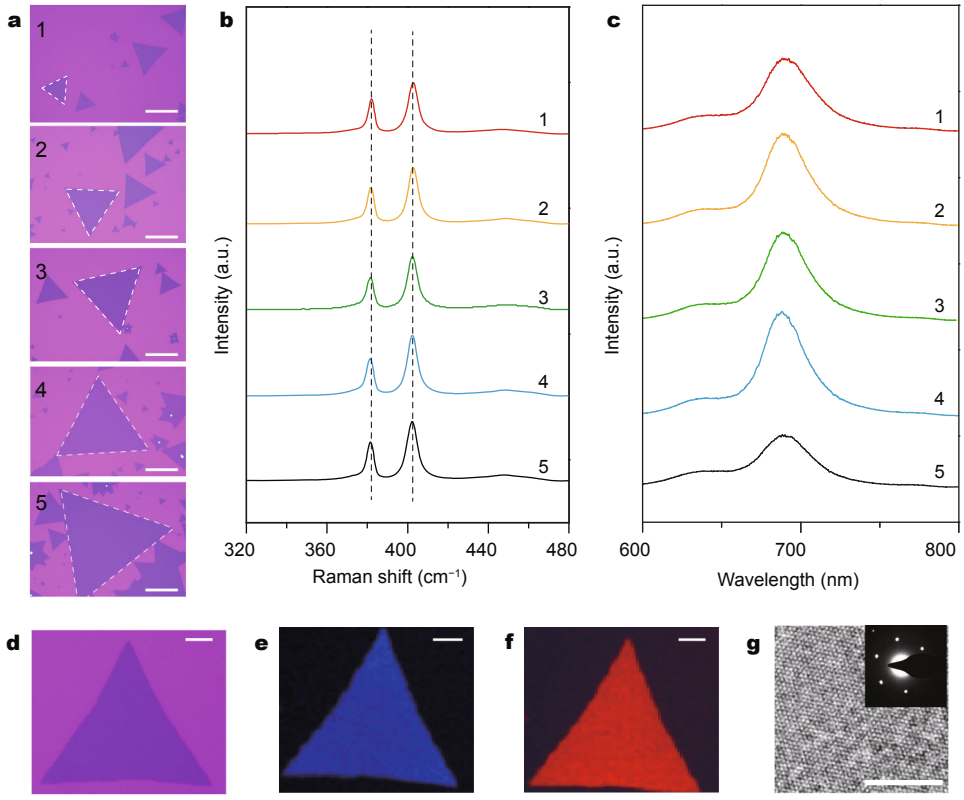


**Figure 3** Raman and PL spectroscopy characterization of the as-synthesized monolayer $MoS_2$ triangles with different sizes. (a) Optical images of the monolayer $MoS_2$ triangles of different sizes marked with dashed white triangles. The scale bar is 100 μm. (b) Raman spectra recorded from the five $MoS_2$ triangles presented in (a). The gaps between the two characteristic peaks are 20.5 $cm^{-1}$. (c) PL spectra recorded from the five $MoS_2$ triangles presented in (a), showing the characteristic peaks at 680 nm. (d) A typical optical image of a monolayer $MoS_2$ triangle and its corresponding Raman intensity mapping (e) at the 402.5 $cm^{-1}$. PL intensity mapping (f) at the wavelength of 680 nm. The scale bars are 10 μm. (g) High-resolution TEM image of the as-grown $MoS_2$ triangle, with inset diffraction pattern. The scale bar is 5 nm.

triangles. In order to investigate the crystal structure of the as-grown $MoS_2$ samples, high-resolution TEM was utilized to analyze the crystal structure of the $MoS_2$ triangles. As shown in Fig. 3g, the TEM results demonstrate that these $MoS_2$ triangular islands are single crystals.

To further evaluate the electronic properties of these as-grown monolayer $MoS_2$ triangles, back-gated FETs were fabricated on the Si substrate with 300 nm of $SiO_2$. The source and drain electrodes were defined by E-beam lithography and 5 nm Ti/50 nm Au were deposited onto the surface through E-beam evaporation subsequently. A typical transfer and output characteristics of the fabricated $MoS_2$ FETs are shown in Figs 4a and b. It can be clearly seen that the $MoS_2$ transistor exhibits an n-type semiconductor behavior, which is in consistent with previous report [5]. The mobility of the $MoS_2$ FETs was calculated using the equation [35]

$$\mu = \frac{\mathrm{d}I_{\mathrm{ds}}}{\mathrm{d}V_{\mathrm{g}}} \times \frac{L}{WC_0V_{\mathrm{ds}}},$$

where $L$ and $W$ are the length and width of the $MoS_2$ channel, and $C_0$ is the capacitance per unit area of the $SiO_2$ layer. The calculated carrier mobility of the $MoS_2$ FET was ~21.8 $cm^2\ V^{-1}\ s^{-1}$, suggesting excellent transporting property compared with previously reported back-gated FETs fabricated by CVD grown monolayer $MoS_2$ [6,22,25].

Moreover, the obtained drain current on/off ratio of our device is up to $10^7$, which is also higher than the previously reported value. These excellent electronic properties further confirm that the as-grown monolayer $MoS_2$ triangles are nearly perfect single crystals in high uniformity because there are few grain boundaries or other defects scattering the carriers while transporting [31].

After successful characterization of the electronic properties of the $MoS_2$ device, a laser with wavelength of 550 nm was employed to investigate its photoresponse. Figs 5a and c show the transfer and output characteristics of the $MoS_2$ device under the laser illumination. The photocurrent can be calculated using $I_{\mathrm{ph}} = I_{\mathrm{illuminated}} - I_{\mathrm{dark}}$. According to the result in Figs 5b and c, the calculated photocurrent of the device is about $7 \times 10^{-7}$ A. While the incident laser power was 20 mW $mm^{-2}$, the calculated photoresponsivity is 7 A $W^{-1}$ at a −15 V gate voltage and a 1 V drain voltage. The time-resolved photo-response of the monolayer $MoS_2$ FET measured by alternatively switching on and off of the laser illumination is shown in Fig. 5d. As can be clearly seen, when exposed to the 550 nm laser, the drain current $I_{\mathrm{ds}}$ increases sharply and gets stabilized at a constant value; when the laser is cut off, the drain current $I_{\mathrm{ds}}$ drops down to the original value immediately. The response time of the device was about 20 ms and the recovery time was about 55 ms (Fig. S2), which indicates that the photoresponse performance of the as-grown $MoS_2$ is excellent for photodetector [7,35].

## CONCLUSIONS

In summary, we have systematically studied the growth mechanism of monolayer $MoS_2$ and controlled synthesized high quality monolayer $MoS_2$ single crystals with the edge size up to 405 μm on $SiO_2$/Si substrate. The Raman and PL spectroscopy results demonstrate that the as-synthesized monolayers are highly homogeneous. The electronic and photoresponse properties of the monolayer $MoS_2$ single crystals were evaluated using back-gated FETs. The average carrier mobility of the $MoS_2$ is about 21.8 $cm^2\ V^{-1}\ s^{-1}$, and the on/off ratio is up to $10^7$, fairly good compared to previously reported $MoS_2$ monolayer back-gated FETs. The response time upon a 550 nm laser is less than 20 ms. Moreover, the introduced controlled synthesis method of large area $MoS_2$ monolayer single crystals with high mo-

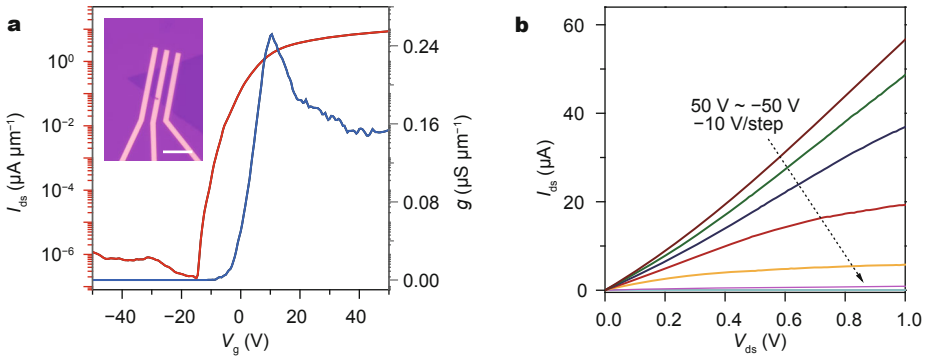


**Figure 4** Electrical characterizations of the as-grown $MoS_2$ back-gated FETs. (a) Transfer characteristic of typical $MoS_2$ FETs at the drain voltage of 0.2 V. The inset is an optical image of the monolayer $MoS_2$ transistor. The scale bar is 10 μm. (b) The $I_{ds}$-$V_{ds}$ output characteristic curves of the $MoS_2$ transistor measured under ambient condition.

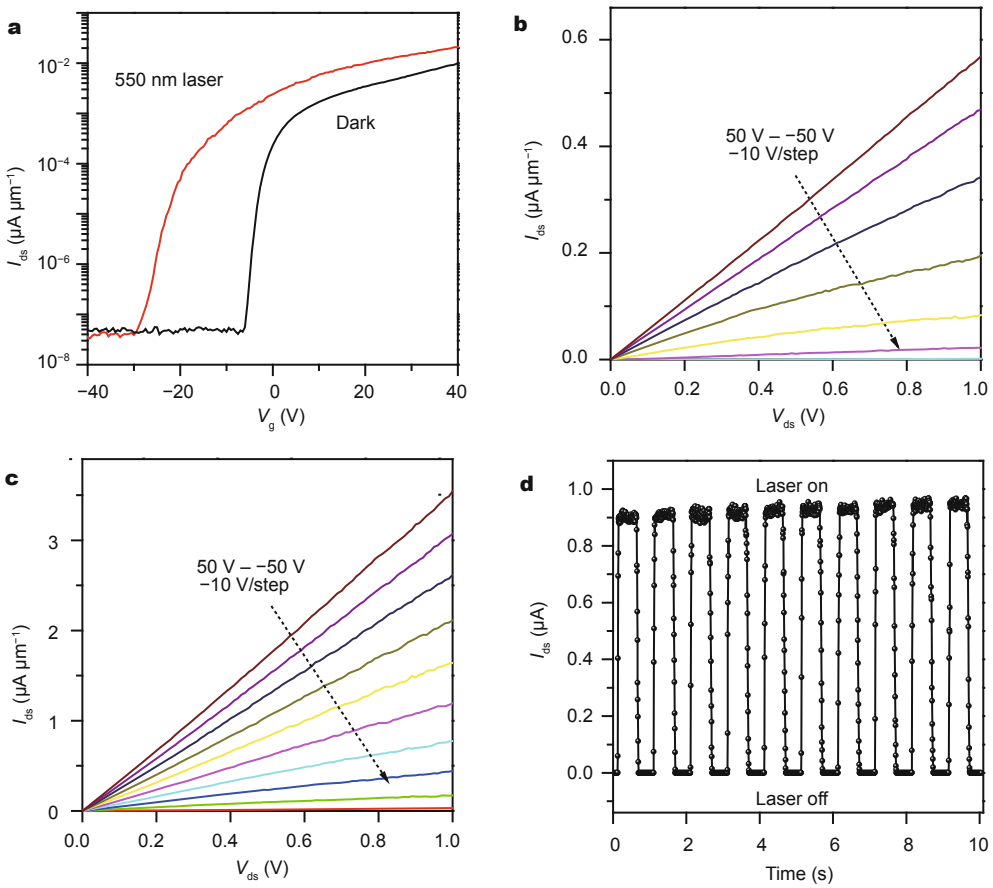


**Figure 5** Photo-response measurements of the back-gated $MoS_2$ FETs. (a) Room temperature transfer curves of the monolayer $MoS_2$ transistor at the drain voltage of 0.01 V. The black curve was measured under dark condition, and the red curve was measured under 550 nm laser illuminated condition. (b) The $I_{ds}$-$V_{ds}$ output characteristic curves of the $MoS_2$ transistor measured under dark condition and (c) under a 550 nm laser illuminated condition. The gate voltage ranges from 50 to −50 V. (d) Time-resolved photo-response of the monolayer $MoS_2$ transistor measured by alternatively switching on and off of the laser illumination.

bility and fast photoresponse may pave the way for future applications in optoelectronics devices.

**Received 29 February 2016; accepted 19 March 2016; published online 29 March 2016**


1 Fiori G, Bonaccorso F, Iannaccone G, *et al.* Electronics based on two-dimensional materials. Nat Nanotechnol, 2014, 9: 768–779
2 Bernardi M, Palummo M, Grossman JC. Extraordinary sunlight absorption and one nanometer thick photovoltaics using two-dimensional monolayer materials. Nano Lett, 2013, 13: 3664–3670
3 Eda G, Maier SA. Two-dimensional crystals: managing light for optoelectronics. ACS Nano, 2013, 7: 5660–5665
4 Radisavljevic B, Whitwick MB, Kis A. Integrated circuits and logic operations based on single-layer $MoS_2$. ACS Nano, 2011, 5: 9934–9938
5 Radisavljevic B, Radenovic A, Brivio J, Giacometti V, Kis A. Single-layer $MoS_2$ transistors. Nat Nanotechnol, 2011, 6: 147–150
6 Schmidt H, Wang S, Chu L, *et al.* Transport properties of monolayer $MoS_2$ grown by chemical vapor deposition. Nano Lett, 2014, 14: 1909–1913
7 Lopez-Sanchez O, Lembke D, Kayci M, Radenovic A, Kis A. Ultrasensitive photodetectors based on monolayer $MoS_2$. Nat Nanotechnol, 2013, 8: 497–501
8 Wu S, Huang C, Aivazian G, *et al.* Vapor-solid growth of high optical quality $MoS_2$ monolayers with near-unity valley polarization. ACS Nano, 2013, 7: 2768–2772
9 Zhang J, Najmaei S, Lin H, Lou J. $MoS_2$ atomic layers with artificial active edge sites as transparent counter electrodes for improved performance of dye-sensitized solar cells. Nanoscale, 2014, 6: 5279–5283
10 Wu W, Wang L, Li Y, *et al.* Piezoelectricity of single-atomic-layer $MoS_2$ for energy conversion and piezotronics. Nature, 2014, 514: 470–474
11 Cho B, Hahm MG, Choi M, *et al.* Charge-transfer-based gas sensing using atomic-layer $MoS_2$. Sci Rep, 2015, 5: 8052
12 Liu K, Yan Q, Chen M, *et al.* Elastic properties of chemical-vapor-deposited monolayer $MoS_2$, $WS_2$, and their bilayer heterostructures. Nano Lett, 2014, 14: 5097–5103
13 Liu B, Chen L, Liu G, *et al.* High-performance chemical sensing using schottky-contacted chemical vapor deposition grown mono layer $MoS_2$ transistors. ACS Nano, 2014, 8, 5304–5314
14 Late D, Liu B, Matte H, Dravid V, Rao C. Hysteresis in single-layer

$MoS_2$ field effect transistors. ACS Nano, 2012, 6: 5635–5641
15 Late D, Huang Y, Liu B, *et al.* Sensing behavior of atomically thin-layered $MoS_2$ transistors. ACS Nano 2013, 7: 4879–4891
16 Zhan Y, Liu Z, Najmaei S, Ajayan P, Lou J. Large-area vapor-phase growth and characterization of $MoS_2$ atomic layers on a $SiO_2$ substrate. Small, 2012, 8: 966–971
17 Van der Zande M, Huang Y, Chenet A, *et al.* Grains and grain boundaries in highly crystalline monolayer molybdenum disulphide. Nat Mater, 2013, 12: 554–561
18 Kim S, Sangwan K, Jariwala D, *et al.* Influence of stoichiometry on the optical and electrical properties of chemical vapor deposition derived $MoS_2$. ACS Nano, 2014, 8: 10551–10558
19 Shi Y, Li H, Li J. Recent advances in controlled synthesis of two-dimensional transition metal dichalcogenides via vapour deposition techniques. Chem Soc Rev, 2015, 44: 2744–2756
20 Liu Z, Amani M, Najmaei S, *et al.* Strain and structure heterogeneity in $MoS_2$ atomic layers grown by chemical vapour deposition. Nat Commun, 2014, 5: 5246
21 Najmaei S, Liu Z, Zhou W, *et al.* Vapour phase growth and grain boundary structure of molybdenum disulphide atomic layers. Nat Mater, 2013, 12: 754–759
22 Amani M, Chin L, Birdwell G, *et al.* Electrical performance of monolayer $MoS_2$ field-effect transistors prepared by chemical vapor deposition. Appl Phys Lett, 2013, 102: 193107
23 Jeon J, Jang K, Jeon M, *et al.* Layer-controlled CVD growth of large-area two-dimensional $MoS_2$ films. Nanoscale, 2015, 7: 1688–1695
24 Ling X, Lee H, Lin Y, *et al.* Role of the seeding promoter in $MoS_2$ growth by chemical vapor deposition. Nano Lett, 2014: 14, 464–472
25 Zhang J, Yu H, Chen W, *et al.* Scalable growth of high-quality polycrystalline $MoS_2$ monolayers on $SiO_2$ with tunable grain sizes. ACS Nano, 2014, 8: 6024–6030
26 Wang S, Rong Y, Fan Y, *et al.* Shape evolution of monolayer $MoS_2$ crystals grown by chemical vapor deposition. Chem Mat, 2014, 26: 6371–6379
27 Lee H, Zhang Q, Zhang W, *et al.* Synthesis of large-area $MoS_2$ atomic layers with chemical vapor deposition. Adv Mater, 2012, 24: 2320–2325
28 Ji Q, Zhang Y, Zhang Y, Liu Z. Chemical vapour deposition of group-VIB metal dichalcogenide monolayers: engineered substrates from amorphous to single crystalline. Chem Soc Rev, 2015, 44: 2587–2602
29 Balendhran S, Ou Z, Bhaskaran M, *et al.* Atomically thin layers of $MoS_2$ via a two step thermal evaporation-exfoliation method. Nanoscale, 2012, 4: 461–466
30 Duan X, Wang C, Shaw C, *et al.* Lateral epitaxial growth of two-dimensional layered semiconductor heterojunctions. Nat Nanotechnol, 2014, 9: 1024-1030
31 Najmaei S, Amani M, Chin L, *et al.* Electrical transport properties of polycrystalline monolayer molybdenum disulfide. ACS Nano, 2014, 8: 7930–7937
32 Liu L, Fathi M, Chen L, *et al.* Chemical vapor deposition growth of monolayer $WSe_2$ with tunable device characteristics and growth mechanism study. ACS Nano, 2015, 9: 6119–6127
33 Zhou H, Wang C, Shaw C, *et al.* Large area growth and electrical properties of p-type $WSe_2$ atomic layers. Nano Lett, 2015, 15: 709–713
34 Kumar K, Dhar S, Choudhury H, Shivashankar A, Raghavan S. A predictive approach to CVD of crystalline layers of TMDs: the case of $MoS_2$. Nanoscale, 2015, 7: 7802–7810
35 Yin Y, Li H, Zhang H, *et al.* Single-layer $MoS_2$ phototransistors. ACS Nano, 2012, 6: 74–80

**Acknowledgements** This work was supported by the "Thousands Talents" program for pioneer researcher and his innovation team, China; President Funding of the Chinese Academy of Sciences, National Natural Science Foundation of China (51272238, 21321062, 51432005, and 61405040), Beijing Municipal Science & Technology Commission (Z131100006013004 and Z131100006013005), and Beijing City Committee of Science and Technology (Z151100003315010).

**Author contributions** Pan C and Li Q supervised the project. Yang X and Li Q synthesized the monolayer $MoS_2$ samples, designed and performed the experiments, analyzed the results and wrote the manuscript. Wang Z and Hu G helped with the monolayer $MoS_2$ synthesis. Yang Z and Liu X assisted in the device fabrication and measurement. Dong M contributed to the data analysis. All authors contributed to the general discussion.

**Conflict of interest** The authors declare that they have no conflict of interest.

**Supplementary information** Supporting data are available in the online version of the paper.

**Xiaonian Yang** is a master student since 2014 under the guidance of Prof. Caofeng Pan at Beijing Institute of Nanoenergy and Nanosystems, Chinese Academy of Sciences, China. She received her BSc degree at the School of Materials Science and Engineering, Huazhong University of Science and Technology in 2014. Her current research concentrates on two-dimensional materials growth, corresponding device fabrication and their applications in nanoelectronics.

**Qiang Li** received his PhD degree in 2014 from Aarhus University, Denmark. Currently, he is a postdoctoral researcher at the Bio-SPM group, Aarhus University. His current research focuses on the development of novel atomic force microscope technique for probing the physical and chemical properties of new functional materials at the nanoscale.

**Guofeng Hu** received the BSc degree at the School of Science from Tianjin Polytechnic University, China, in 2010. He is currently pursuing his PhD degree at the Laboratory of Piezo-phototronics, Beijing Institute of Nanoenergy and Nanosystems, Chinese Academy of Sciences. His research work is focused on the fields of piezotronics/piezo-phototronics for fabricating new electronic and optoelectronic devices.

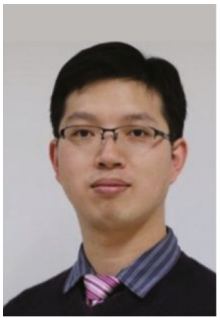

**Caofeng Pan** received his BSc (2005) and PhD (2010) degrees in materials science and engineering from Tsinghua University, China. He then joined Prof. Zhong-Lin Wang's group at Georgia Institute of Technology as a postdoctoral fellow. He is currently a professor and a group leader at Beijing Institute of Nanoenergy and Nanosystems, Chinese Academy of Science since 2013. His main research interests focus on the fields of piezotronics/piezo-phototronics for fabricating new electronic and optoelectronic devices, nano-power source (such as nanofuel cell, nano biofuel cell and nanogenerator), hybrid nanogenerators, and self-powdered nanosystems. He has published over 50 peer reviewed papers, with citation over 1000 and H-index of 19. Details can be found at http://piezotronics. binn.cas.cn/.

## 高质量单层$MoS_2$的可控合成及其在微纳电子方面的应用

杨小年, 李强, 胡国锋, 王泽高, 杨振宇, 刘兴强, 董明东, 潘曹峰

**摘要** 二维层状材料由于其在光电器件方面的潜在应用引起了广泛关注, 二硫化钼 ($MoS_2$) 是其中研究最多的材料之一. 单层二硫化钼可通过机械剥离或者化学气相合成的方法制备, 但是与石墨烯相比, 大面积且高质量的单层二硫化钼单晶的可控合成仍然有待提高. 本文报道了一种可控合成大面积高质量单层$MoS_2$单晶的方法, 合成出了边长达405 μm的单层二硫化钼三角形. 对产物进行了光谱表征, 结果表明其光学性质十分均匀, 透射电镜表征结果表明产物是单晶结构. 基于单层$MoS_2$的场效应晶体管 (FET) 表现出良好的电学性能, 其载流子迁移率高达21.8 $cm^2 V^{-1} s^{-1}$, 光响应度为7 A $W^{-1}$, 响应时间仅为20 ms. 此合成方法使单层$MoS_2$的制备更加简易可靠, 可促进其进一步研究及应用.